International Journal of Pharmaceutics 382 (2009) 205–214

Contents lists available at ScienceDirect

International Journal of Pharmaceutics

journal homepage: www.elsevier.com/locate/ijpharm

Pharmaceutical Nanotechnology

Ionically crosslinked chitosan/tripolyphosphate nanoparticles for oligonucleotide and plasmid DNA delivery

Noemi Csaba, Magnus Köping-Höggård, Maria Jose Alonso*

Department of Pharmacy and Pharmaceutical Technology, School of Pharmacy, University of Santiago de Compostela, 15782 Santiago de Compostela, Spain

ARTICLE INFO

Article history:
Received 5 May 2009
Received in revised form 23 July 2009
Accepted 26 July 2009
Available online 4 August 2009

Keywords:
Chitosan
Gene delivery
Nanoparticles
Oligonucleotides
pDNA
Ionic gelation

ABSTRACT

Ionically crosslinked nanoparticles based on high and low molecular weight chitosans (CS) were formulated with plasmid DNA or dsDNA oligomers using the ionic gelation technique with pentasodium tripolyphospate (TPP) as crosslinking agent. The resulting CS/TPP nanoparticles were investigated with regard to their physical–chemical properties, *in vitro* transfection efficiency, toxicity, cellular uptake, and *in vivo* gene expression following intratracheal administration to mice. The effects of co-formulating the nanoparticles with a model protein, BSA, were also studied. CS/TPP nanoparticles showed high encapsulation efficiencies both for plasmid DNA and dsDNA oligomers (20-mers), independent of CS molecular weight. TEM images revealed a spherical shape of the CS/TPP nanoparticles in contrast to the heterogeneous and irregular morphology displayed by conventional chitosan polyplexes. The nanoparticles showed high physical stability and no DNA release could be detected in diverse release media, nor even after incubation with heparin. Low molecular weight (LMW) CS/TPP nanoparticles gave high gene expression levels in HEK 293 cells already 2 days after transfection, reaching a plateau of sustained and high gene expression between 4 and 10 days. The inclusion of BSA into the nanostructures did not alter the inherent transfection efficiency of the nanoparticles. Confocal studies suggest endocytotic cellular uptake of the nanoparticles and a subsequent release into the cytoplasm within 14 h. LMW CS/TPP nanoparticles mediated a strong beta-galactosidase expression *in vivo* after intratracheal administration. The results of this study forward ionically crosslinked CS/TPP nanoparticles as a biocompatible non-viral gene delivery system and generate a solid ground for further optimization studies, for example with regard to steric stabilization and targeting.

1. Introduction

Chitosan and its derivatives have emerged as a promising vehicles for non-viral plasmid DNA (pDNA) delivery during in the past decade (Morille et al., 2008; Dang and Leong, 2006; Leong et al., 1998; Mansouri et al., 2004). More recently, chitosan-based delivery systems have also shown potential for nasal delivery of siRNA and subsequent gene interference in the lung mucosa (Howard et al., 2006, 2008; Liu et al., 2007).

Most commonly, these gene delivery systems consist of ionic complexes, i.e. polyplexes, which are assembled mainly through ionic interactions between the positively charged primary amino groups of chitosan and the negatively charged phosphate groups of pDNA. As a result, and in agreement with the theories underlying polyelectrolyte interactions, the ability of chitosan to form polyplexes with pDNA is highly dependent on two structural parameters: the degree of deacetylation (i.e. positive charge density) and the molecular weight (Koping-Hoggard et al., 2001, 2003, 2004). For example, studies have shown that at least 2 out of 3 chitosan monomers should carry a primary amino group (i.e. be deacetylated) in order to form polyplexes enabling gene expression *in vitro* and after mucosal administration *in vivo* (Koping-Hoggard et al., 2001). Furthermore, the formation of polyplexes is favoured as the molecular weight of chitosan increases. In contrast, with regard to their transfection efficiency, polyplexes based on low molecular weight chitosans were found to be preferable than those of high molecular weights (Koping-Hoggard et al., 2003, 2004; Danielsen et al., 2004). Indeed, low molecular weight chitosan (3–10 kDa) polyplexes have been reported to be as efficient as polyplexes based on polyethylenimine (PEI), one of the most efficient non-viral gene delivery vehicles (Koping-Hoggard et al., 2004).

Although chitosan polyplexes are promising "*in vitro*" transfecting agents, they still suffer from several limitations as mucosal gene carriers like: (i) difficulty of isolation and long term storage, (ii) dissociation of the complexes in the presence of polyanions, (iii) undefined physical shapes, (iv) limited capacity to co-associate other functional molecules, such as proteins, to the polyplex structure that could help to overcome the cellular barriers for efficient

* Corresponding author. Tel.: +34 981 594488x14885; fax: +34 981 547148.
E-mail address: mariaj.alonso@usc.es (M.J. Alonso).

0378-5173/$ – see front matter © 2009 Elsevier B.V. All rights reserved.
doi:10.1016/j.ijpharm.2009.07.028

gene transfer and expression. Furthermore, the formation of the nanoparticulate structure is highly dependent on the presence of DNA as counter anion.

One alternative strategy previously tested to associate DNA to chitosan has been based on the addition of a desolvating agent, typically sodium-sulfate, which induces phase separation and the formation of nanoparticles (Leong et al., 1998). Nanoparticles prepared by this desolvation method exhibited transfection efficiency values that were comparable to those observed for chitosan polyplexes. Furthermore, another report has indicated that the efficacy of these nanoparticles could be further enhanced by co-formulating pDNA with an endosomolytic polymer, i.e. poly(propyl acrylic acid) (Kiang et al., 2004). Other approaches to improve the efficacy of the more classical pDNA–chitosan complexes have been based on the chemical modification of chitosan with a hydrophobic segment, thus enabling the self-aggregation of chitosan in aqueous media (Kim et al., 2001; Yoo et al., 2005). Additionally, the covalent or ionic crosslinking of pre-formed pDNA–chitosan complexes has also been reported. In this latter case the increased gene expression was attributed to the extended release time and sustained gene expression as a direct consequence of the more compact, crosslinked polymer matrix (Lee et al., 2007; Dung et al., 2007).

As an alternative to these previously developed chitosan-based pDNA nanocarriers, the present work was intended to entrap pDNA into reticulated chitosan nanoparticles obtained by ionic gelation. This technique involves the addition of a crosslinking agent, i.e. tripolyphosphate (TPP), into the aqueous phase containing chitosan, thus leading to the formation of chitosan nanogels (Calvo et al., 1997b). This technique has been previously adapted for the encapsulation of peptides and proteins (Calvo et al., 1997a,b; Cuna et al., 2006; Fernandez-Urrusuno et al., 1999a; Vila et al., 2002). As compared to the other methods used for DNA association, the nanoparticle formation is not only determined by the electrostatic interactions between chitosan and DNA, but simultaneously also by physical entrapment upon the ionic crosslinking induced by TPP. This process results in the controlled gelation of chitosan in the form of spherical, homogeneous and compact nanoparticles, characteristics that are expected to benefit the performance of the system both *in vitro* and *in vivo*.

The aim of this study was to adapt the ionic gelation technique for the encapsulation of different nucleic acids (plasmid DNA and short oligonucleotides) into chitosan nanoparticles and to evaluate their potential as gene delivery nanocarriers. The physical–chemical properties of chitosan nanoparticles were optimized by studying the influence of several key parameters including (i) CS concentration, (ii) CS molecular weight (i.e. 10 kDa vs. 125 kDa), (iii) CS/TPP polymer ratio and (iv) DNA loading. Moreover, the possibility to co-encapsulate a protein that could confer additional advantages to the nanoparticles such as improving the cell internalization or the intracellular trafficking of the DNA, was also investigated. The transfection efficiency of CS/TPP nanoparticles was evaluated in cell cultures and *in vivo*, following intratracheal administration in mice. Finally, mechanistic studies aimed at exploring the internalization of the nanoparticles into the cells were also performed.

2. Materials and methods

2.1. Materials

Ultrapure chitosan hydrochloride salt Protasan UP CL 113 with $M_n = 5.4 \times 10^4$, $M_w = 8.0 \times 10^4$ as determined by SEC-MALLS (Lamarque et al., 2005; Csaba et al., 2009) and with 14% acetylation degree as determined by ^{1}H NMR (Fernandez-Megia et al., 2005) was purchased from Pronova Biomedical A.S. (Norway). Plasmid DNA (pDNA) encoding green fluorescent protein (pEGFP-C1) and pDNA encoding beta-galactosidase (pCMVβ-Gal) driven by a CMV promoter were purchased from Elim Biopharmaceuticals (San Francisco, CA, USA). Double stranded 20-mer DNA oligomers (upper sequence: 5′-acgaagctgtagcgtgtacaT T-3′; lower sequence: 5′-tgtacacgctacagcttcgtT T-3′) were obtained from Biospring (Frankfurt, Germany). Pentasodium tripolyphosphate (TPP), bovine serum albumin (BSA), heparin, sulforhodamine 101 acid chloride and ethidium bromide (purity 95%) were obtained from Sigma–Aldrich (Madrid, Spain). One kBp DNA ladder was obtained from Life Technologies (Barcelona, Spain). All other solvents and chemicals were of the highest grade commercially available. Animal experiments were carried out with the approval of the Ethical Committee of the Faculty of Medicine, University of Santiago de Compostela. Male Balb/c mice from the Central Animals House of the University of Santiago de Compostela were used. The animals were kept in a 12 h light/dark cycle and they were allowed to access food and water ad libitum.

2.2. Depolymerization of chitosan

Chitosan oligomers were generated by sodium nitrite degradation as previously described (Janes and Alonso, 2003). Briefly, varying quantities of 0.1% (w/v) $NaNO_2$ (Probus S.A., Barcelona, Spain) were added to the chitosan solution (2 mg/ml) at room temperature under magnetic stirring, and the reaction was left overnight to assure completion of the degradation. We have previously simulated the depolymerization process of chitosan using Matlab 5.1 (MathWorks, Inc., USA). With this program, the necessary amount of $NaNO_2$ could be predicted in order to obtain an approximate Mw of 10 kDa. Accordingly, the resulting product had $M_n = 8.9 \times 10^3$ and $M_w = 1.2 \times 10^4$ values as determined by SEC-MALLS (Lamarque et al., 2005; Csaba et al., 2009).

2.3. Preparation of FITC-labelled plasmid and sulforhodamine-labelled chitosan

The preparation of FITC-labelled plasmid was performed as described previously (Ishii et al., 2000). Briefly, fluorescein-5-isothiocyanate was reacted overnight with 2-(4-aminophenyl)-ethylamine in dimethyl-formamide under stirring at 25 °C. The formation of FITC-aniline was monitored by thin layer chromatography. Then, FITC-aniline was reacted with sodium nitrite in 0.5 M HCl at 0 °C under stirring. The reaction was stopped by the addition of 1 M NaOH and subsequently, the obtained FITC-diazonium solution was mixed with pCMVβ-Gal plasmid in 0.1 M borate buffer (pH 9) at 25 °C, under stirring. The obtained FITC-plasmid was purified by ethanol precipitation and by gel exclusion chromatography using PD 10 desalting columns with Sephadex G-25 (Amersham Biosciences, Spain).

Chitosan was labelled with sulforhodamine according to the method described by Ishii et al. (2000). Chitosan (10 and 125 kDa) and sulforhodamine 101 acid chloride were dissolved separately in ultapure water adjusted at pH 7.2 adjusted with 0.1 N NaOH. The solutions were mixed and the reaction was carried out overnight at 20 °C under stirring. In order to purify the product, 5 ml of ethanol was added to the reaction mixtures. Next, a few drops of 1N NaOH solution were added to the solution in order to precipitate the product. After centrifugation (6000 RCF for 10 min), the supernatant was discarded and the product was redissolved in 5 ml of ultrapure water and a few drops of 1N HCl. The purification process was repeated 5 times, until fluorescence could not be detected in the supernatant. The sulforhodamine-labelled chitosan was then stored in a freeze-dried form.

2.4. Preparation and physicochemical characterization of CS/TPP nanoparticles

CS/TPP nanoparticles were prepared according to the ionotropic gelation technique previously developed by our group (Calvo et al., 1997a). Chitosan and tripolyphosphate were separately dissolved in ultrapure water at different concentrations in order to obtain CS/TPP ratios 6/1, 5/1 and 4/1. Nanoparticles were formed instantaneously upon the dropwise addition of a fixed volume of TPP (e.g. 1.2 ml) solution to a fixed volume of chitosan solution (e.g. 3 ml) under magnetic stirring. For their further characterisation, nanoparticles were concentrated by centrifugation at 10,000 RCF on a 10 μl glycerol bed (Avanti 30 Beckman, Barcelona, Spain) and were resuspended in ultrapure water.

Mean particle size and polydispersion index were determined by photon correlation spectroscopy (PCS). Samples were diluted with freshly filtered ultrapure water and PCS analysis was performed at 25 °C with an angle detection of 90°. Particle size was calculated by the Brownian movement of the nanoparticles by using the Stokes–Einstein equation (Zetasizer 3000HS, Malvern Instruments, Malvern, U.K.).

The zeta potential values were calculated from the mean electrophoretic mobility of the particles as determined by laser-Doppler anemometry (LDA). As recommended by the manufacturers instructions, samples were diluted with a weak electrolyte (1 mM KCl) in order to provide constant conductivity and ionic strength. Zeta potential values were calculated from electrophoretic mobility data by using the equation of Henry (Zetasizer 3000HS, Malvern Instruments, Malvern, U.K.). In all cases, mean values were obtained from the analysis of three different batches, each of them measured three times.

The morphology of the nanoparticles was examined by transmission electron microscopy (CM 12 Philips, Eindhoven, The Netherlands) using samples stained with a 2% phosphotungstic acid solution.

2.5. Encapsulation of plasmid DNA, dsDNA oligomers and BSA

For their encapsulation, pDNA or small dsDNA oligonucleotides were incorporated into the TPP solution prior to nanoparticle formation. The theoretical DNA loadings were 5, 10 or 20% with respect to the total amount of CS used for particle preparation.

Chitosan–pDNA complexes (polyplexes) made from the low molecular weight CS were used as control and were formed at a charge ratio of 10:1 (+/−) as previously described (Koping-Hoggard et al., 2003). Briefly, polyplexes were formulated by adding chitosan and then pDNA stock solutions to ultrapure water, under intense stirring on a vortex mixer. The charge ratio was defined as the ratio between the maximum number of protonable primary amines in chitosan and the number of negative phosphates on pDNA. Polyplexes were produced at a constant pDNA concentration of 13.3 μg/ml for the *in vitro* studies (gel retardation assays and transfection experiments) and at a pDNA concentration of 50 μg/ml for use in the *in vivo* studies.

For its encapsulation, bovine serum albumin (BSA) was incorporated into the TPP solution prior to nanoparticle formation. The theoretical loading was 30% with respect to the total amount of CS used for particle preparation.

2.6. Loading capacity of CS/TPP nanoparticles

Encapsulation efficiencies of plasmid DNA, dsDNA oligomers and BSA were calculated from the amount of non-encapsulated material recovered in the supernatant samples collected upon centrifugation of the nanoparticles (10,000 RFC, 40 min). The amount of recovered DNA was determined by fluorimetry (LS 50B luminescence spectrometer, Perkin-Elmer) using PicoGreen® reagent (Molecular Probes, OR, USA). The amount of BSA was determined by the standard microBCA protein assay (Pierce, Rockford, USA), using supernatants of the corresponding blank formulations for the calibration curves.

Additionally, the association of DNA to the nanoparticles was also determined by gel electrophoresis assays (1% agarose containing ethidium bromide, 50 V, 120 min, Sub-Cell GT 96/192, Bio-Rad Laboratories Ltd., England).

2.7. In vitro release of DNA

Plasmid DNA release was determined by incubating the nanoparticles in pH 4 and 7.4 acetate buffer or in ultrapure water (37 °C, horizontal shaking 100–110 cycles min^{-1}). At time intervals of 1 day and 1, 2, 3, 4 weeks, individual samples were isolated by centrifugation (10,000 RCF, 40 min). Supernatant samples were analyzed by agarose gel electrophoresis using unencapsulated pEGFP-C1 plasmid as positive control sample. DNA release was also studied by agarose gel electrophoresis assay after incubating the nanoparticles and polyplexes with 5 μg/ml heparin for 1 and 4 h (Koping-Hoggard et al., 2004).

2.8. Cell culture experiments

Transfection studies were performed in the HEK 293 cell line 293. The cells were cultivated in Minimum Essential Medium (Sigma–Aldrich, Madrid, Spain) supplemented with 10% fetal bovine serum (Sigma–Aldrich) and maintained at 37 °C; 5% CO_2. The cells were seeded at 70% confluence in 24-well tissue culture plates (Costar, Cambridge, UK) 24 h before the experiments. To transfect the cells, cells were washed and then DNA loaded CS/TPP nanoparticles or corresponding CS–DNA polyplexes were added in 300 μl HBSS pH 6.5. After 5 h incubation, the formulations were removed and 1 ml of fresh culture medium was added. The medium was changed every second day for experiments that exceeded 2 days. At the indicated time points, cells were investigated under a fluorescence microscope (Nikon eclipse TE2000-S, Nikon UK Ltd., UK) and counted for GFP-positive cells using Adobe Photoshop Elements.

2.9. Cytotoxicity studies

Cells were seeded at 70% confluency in 96-well tissue culture plates (Costar) 20–24 h before incubating the cells with increasing concentrations of pDNA-loaded CS/TPP nanoparticles and CS–pDNA polyplexes. After 1 h incubation, the formulations were removed and the cells were assayed for viability using the MTS assay as previously described (Csaba et al., 2005). In another set of experiments, the cells were allowed to recover for 24 h after removal of the formulations, before being assayed for viability.

2.10. Uptake and intracellular distribution of CS/TPP nanoparticles

To observe the cellular uptake and intracellular distribution of CS/TPP nanoparticles, cells were seeded at 70% confluency on sterile glass covers inserted in the wells of 24-well tissue culture plates (Costar). Nanoparticles containing fluorescently labelled pDNA were formulated and incubated with the cells according to the procedures described previously in Sections 2.5 and 2.8. After their incubation, the cells were rinsed with PBS pH 7.4, fixed (3.5% paraformaldehyde/60 mM saccharose in PBS), mounted and examined under a confocal scanning laser microscope (Leica TCS-SP2, Leica Microsystems, Germany). In another set of experiments, the cells were incubated for another 15 h after removal of the

nanoparticles. The cells were processed as described above with the addition that the cells were permeabilized with Triton-X (0.1 M in PBS) and the nuclei of the cells were stained with propidium iodide.

2.11. In vivo gene expression studies

For *in vivo* experiments, Balb/c mice were anaesthetized with pentobarbital and the trachea was surgically exposed by a 0.5 cm long skin incision in the neck. Administration was performed by slowly injecting pCMV-βGal encapsulated in CS/TPP nanoparticles or naked pCMV-βGal (dose corresponding to 10 μg pDNA in 100 μl) into the trachea with a 28 G needle. The expression of beta-galactosidase was studied 72 h after administration by 5-bromo-4-chloro-3-indolyl-β-D-galactopyranoside (X-gal) histochemistry as described previously (Koping-Hoggard et al., 2001).

2.12. Statistical analysis

Statistical analysis of the experimental data was performed by applying one-way ANOVA tests using the software package SPSS 12.0. Statistical differences are denoted as $^{*}P < 0.05$, $^{**}P < 0.01$ and $^{***}P < 0.001$, respectively. NS = no significant difference ($P > 0.05$).

3. Results and discussion

3.1. Formation and physicochemical characterization of CS/TPP nanoparticles

Initial studies aiming at the optimization of the nanoparticle formation indicated that chitosan concentrations of 1 mg/ml and CS/TPP polymer ratios (w:w) of 4/1–6/1 result in the reproducible formation of nanoparticles with good production yields. The size of the nanoparticles prepared of low molecular weight chitosan (LMW CS/TPP) were smaller, 93 ± 8 nm, than that of nanoparticles prepared of high molecular weight chitosan (HMW CS/TPP, 336 ± 15 nm). The effect of the molecular weight of chitosan on the nanoparticles size can be explained by a decrease in viscosity as the molecular weight decreases and the simultaneously increased ability of LMW CS to form smaller structures. These findings are in agreement with previous results of CS/TPP nanoparticles prepared by ionic gelation (Janes and Alonso, 2003).

3.2. Entrapment of plasmid DNA and BSA

For the loading process, different amounts of plasmid DNA (corresponding to 5, 10 and 20% loadings) were included into the TPP solution prior to nanoparticle formation. This approach differs from that reported by Li et al., where in they adsorbed pDNA onto preformed chitosan nanoparticles. We believe that the entrapment of the pDNA within the CS/TPP nanoparticles would offer several advantages as compared to its surface association: (i) the pDNA would be protected from the potential degradation upon *in vivo* administration; (ii) the surface of the particles could be modified in order to improve their interaction with biological surfaces; (iii) the release process of pDNA would be more controllable by the reticulated particle matrix.

Table 1
Physical–chemical characteristics of low molecular weight (LMW) and high molecular weight (HMW) CS/TPP nanoparticles loaded with pDNA (i.e. pEGFP-C1).

pDNA loading (w/w)	Size (nm)	P.I.	ζ Potential (mV)	E.E. (%)
HMW 5%[a]	278 ± 17	0.340	+40.5 ± 5.6	70.3 ± 6.1
HMW 10%[a]	309 ± 2	0.378	+41.6 ± 0.8	84.9 ± 2.8
HMW 20%[a]	216 ± 7	0.363	+35.2 ± 1.8	94.5 ± 4.1
LMW 5%[b]	109 ± 13	0.109	+10.8 ± 4.2	100
LMW 10%[b]	133 ± 14	0.110	+10.0 ± 2.0	100
LMW 20%[b]	165 ± 10	0.08	+7.7 ± 0.4	100

P.I. = polydispersity index.
E.E. = encapsulation efficiency.
[a] The NP were formed at a chitosan concentration of 1 mg/ml and a CS/TPP ratio of 4:1.
[b] The NP were formed at a chitosan concentration of 1 mg/ml and a CS/TPP ratio of 6:1.

Independent of the chitosan molecular weight, chitosan showed a high efficiency for the encapsulation of pDNA, reaching almost 100% for the formulation with the highest theoretical DNA loading (Table 1). However, HMW CS/TPP nanoparticles had higher positive zeta potential and larger size than the corresponding nanoparticles based on LMW chitosan (Table 1). In general, a small reduction in the zeta potential was observed when the pDNA loading increased. This could be explained by the presence of some negatively charged pDNA on/close to the surface of the nanoparticles.

In order to investigate the possibility of co-encapsulating a protein into CS/TPP nanoparticles together with the pDNA, we chose bovine serum albumin (BSA) as a model protein. The incorporation of 30% BSA into CS/TPP nanoparticles slightly reduced the pDNA loading capacity. This reduction was dependent on the chitosan concentration used for nanoparticle preparation (Table 2). This effect could be attributed to a competition between DNA and BSA in their interaction with chitosan. Despite this competition, the inherent transfection efficiency of these nanoparticles was retained as will be discussed below.

3.3. Encapsulation of oligonucleotides

In a further study we evaluated whether these nanoparticles would be suitable for the encapsulation of much smaller nucleic acid fragments. As shown in Table 3, dsDNA oligomers of 20 monomers in length were efficiently encapsulated into the nanoparticles independent of the chitosan molecular weight. As in the case of pDNA-encapsulation (Table 1), the LMW CS/TPP nanoparticles displayed slightly smaller sizes and lower zeta potentials than HMW CS/TPP nanoparticles. Also, the zeta potential of the nanoparticles decreased as the dsDNA oligomer-loading increased. This suggests that ionically crosslinked CS/TPP nanoparticles would be suitable also for the encapsulation of small antisense oligonucleotides and siRNA, like recently described for similar chitosan–oligonucleotide and chitosan–siRNA complexes (Dung et al., 2007; Howard et al., 2006, 2008).

Table 2
Physical–chemical characteristics of HMW CS/TPP nanoparticles loaded with BSA.

Formulation[a]	Size (nm)	P.I.	ζ Potential (mV)	E.E. BSA (%)	Maximal pDNA loading capacity (w/w)
CS 1 mg/ml NP	268 ± 6	0.373	+32.2 ± 0.8	72.9 ± 4.0	10%
CS 2 mg/ml NP	423 ± 38	0.573	+39.7 ± 0.4	72.6 ± 4.2	5%

P.I. = polydispersity index.
E.E. = encapsulation efficiency.
[a] The nanoparticles were loaded with 30% BSA.

Table 3
Physical–chemical characteristics of low molecular weight (LMW) and high molecular weight (HMW) chitosan nanoparticles loaded with 20-mer oligonucleotides.

Oligo loading (w/w)	Size (nm)	P.I.	ζ Potential (mV)	E.E. (%)
HMW 5%[a]	152 ± 1.7	0.198	+26.4 ± 0.5	56.2 ± 3.3
HMW 10%[a]	195 ± 1.3	0.195	+21.6 ± 0.2	90.7 ± 2.9
HMW 20%[a]	215 ± 4.9	0.290	+19.5 ± 0.1	92.5 ± 5.2
LMW 5%[b]	111 ± 1.2	0.160	+21.5 ± 0.1	66.4 ± 4.6
LMW 10%[b]	122 ± 2.3	0.165	+18.5 ± 0.5	82.5 ± 3.7
LMW 20%[b]	132 ± 2.7	0.166	+14.8 ± 0.3	98.3 ± 1.9

P.I. = polydispersity index.
E.E. = encapsulation efficiency.
[a] The NP were formed at a chitosan concentration of 1 mg/ml and a CS/TPP ratio of 4:1.
[b] The NP were formed at a chitosan concentration of 1 mg/ml and a CS/TPP ratio of 6:1.

3.4. Morphology of CS/TPP nanoparticles

The shape of the pDNA-loaded HMW CS/TPP and LMW CS/TPP nanoparticles was investigated using transmission electron microscopy (TEM). Chitosan–pDNA complexes (polyplexes) based on LMW chitosan were also used as controls, given their reported efficacy for gene delivery (Koping-Hoggard et al., 2004). Independent of the molecular weight, CS/TPP nanoparticles showed a very well defined spherical shape (Fig. 1). In contrast, LMW chitosan polyplexes exhibited some spherical structures, but suffered from rather undefined shapes, indicated by the arrows in Fig. 1. The heterogeneous morphology of chitosan polyplexes obtained in this study agrees with previously reported shapes of chitosan polyplexes (Erbacher et al., 1998; Koping-Hoggard et al., 2003). The differences in shape between nanoparticles and polyplexes may be understood on the basis that the formation of CS/TPP nanoparticles is governed not only by electrostatic interactions between the pDNA and chitosan, but also between TPP and chitosan, the latter interaction being responsible for the controlled gelation of chitosan in a nanoparticulate form. This controlled gelation and reticulation process could explain why the resulting nanoparticles are more spherical and compact than simple complexes. Furthermore, according to previous findings, the shape and size distribution of chitosan nanoparticles could be further improved by the use of chitosans of narrow polymer molecular weight distributions (Zhang et al., 2004). In agreement with the size measurements using photon correlation spectroscopy (Table 1), LMW CS/TPP appeared to be of smaller size on the micrographs than those based on HMW chitosan.

3.5. In vitro release of pDNA from CS/TPP nanoparticles

In order to study the physical stability and the pDNA release properties of CS/TPP nanoparticles, they were incubated in different release media (acetate buffer pH 4 and pH 7.4 or purified water MQ), and assayed in agarose gel retardation assays. As shown in Fig. 2a and b, no DNA release was detected following incubation of pDNA-loaded nanoparticles for up to 1 month, irrespective of the nature of the incubation medium. These results indicate that pDNA is very tightly associated to both HMW and LMW CS/TPP nanoparticles. However, plasmid DNA could be released from the nanoparticles following incubation in acetate buffer in the presence of chitosanase (Fig. 3a). This release behaviour agrees with that previously reported for chitosan nanospheres and polyplexes (Koping-Hoggard et al., 2001; Mao et al., 2001).

Overall, these results show that plasmid DNA is efficiently and tightly associated to the nanoparticles, however, it is not irreversibly bound since it could be released upon the degradation of the polymeric matrix, which is envisaged to occur in a biological environment following *in vivo* administration.

An additional assay was performed in order to evaluate if the associated pDNA could be displaced from CS/TPP nanoparticles. For this purpose, pDNA-loaded nanoparticles were incubated in an aqueous medium containing heparin as a competitive anion. LMW chitosan polyplexes were used as a control, since they are known to be easily dissociated in the presence of heparin (Koping-Hoggard

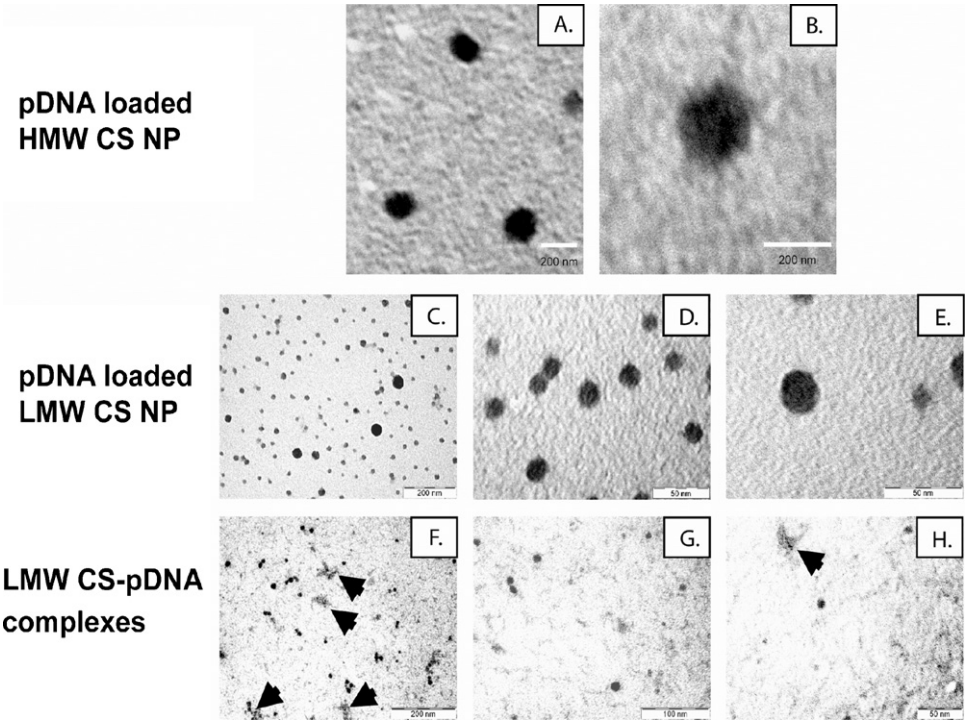

Fig. 1. Morphology of optimized, pDNA-loaded CS/TPP nanoparticles and polyplexes as visualized by transmission electron microscopy (TEM). Scale bars correspond to 200 nm (a, b, c and f), 100 nm (g) and 50 nm (d, e and h), respectively.

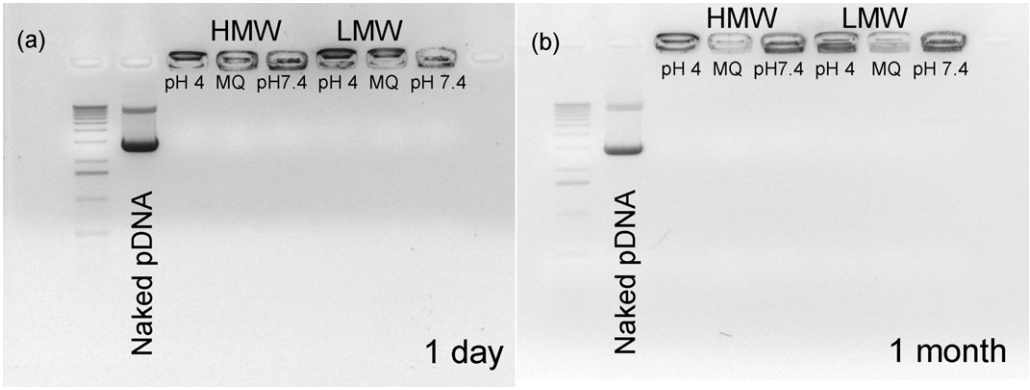

Fig. 2. Agarose gel retardation assays following *in vitro* pDNA release studies from HMW and LMW CS/TPP nanoparticles incubated for (a) 1 day and (b) 1 month. The studies were performed at pH 4 and 7.4 acetate buffer or in ultrapure water (MQ) at 37 °C.

et al., 2004). The results of the electrophoretic analysis (Fig. 3b) showed that, as expected, pDNA is easily displaced from LMW chitosan complexes due to the presence of heparin. This competitive displacement indicates that the plasmid association to chitosan is labile in these polyplexes. Interestingly, this was not the case for pDNA entrapped in nanoparticles, a result that was independent of the chitosan molecular weight (Fig. 3b). This result corroborates that pDNA association to the nanoparticles is not simply mediated by an ionic interaction process, but rather that pDNA is well entrapped within the polymeric mesh formed by the ionically crosslinked chitosan. Thus, the results from the TEM and heparin displacement studies suggest that CS/TPP nanoparticles and chitosan polyplexes differ significantly in the physical entanglement of pDNA into their structures.

3.6. *In vitro transfection efficiency of CS/TPP nanoparticles*

The transfection efficiency of CS/TPP nanoparticles was evaluated in the human embryonic kidney cell line HEK 293, using plasmid DNA encoding green fluorescent protein (GFP). First, we investigated the effect of pDNA loading (5, 10 and 20%) on the efficiency of HMW CS/TPP nanoparticles. A dose of 1 μg pDNA was used in the transfection studies and the number of GFP-transfected cells was monitored for up to 10 days. As shown in Fig. 4a, HMW CS/TPP

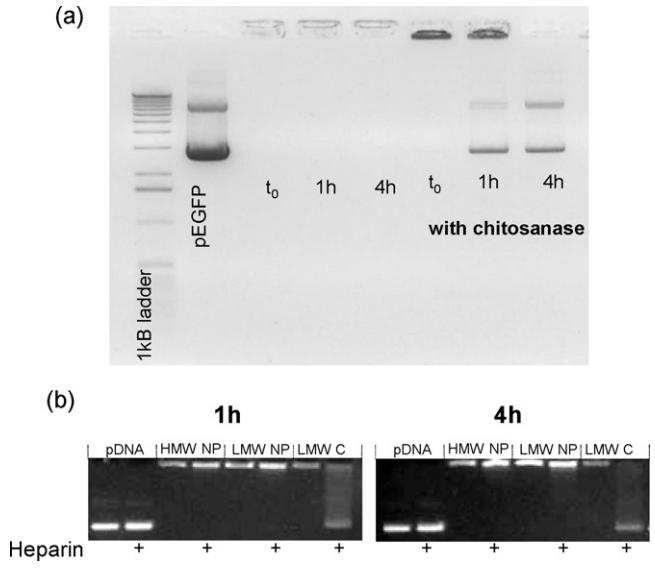

Fig. 3. Agarose gel retardation assays following incubation of CS/TPP nanoparticles and polyplexes with (a) chitosanase, and (b) anionic heparin for 1 and 4 h.

nanoparticles with the highest pDNA loading (20%) resulted in the highest number of transfected cells at all time points investigated, reaching about 25% GFP-positive cells 8 days after transfection. This level of GFP gene expression is in good correlation with that previously was reported for optimized chitosan polyplexes based on HMW chitosan in the same cell line (Koping-Hoggard et al., 2001). Transfection using naked pGFP did not result in any GFP-positive cells (data not shown). Our observation that the gene expression increased with the pDNA loading is interesting since the plasmid dose was constant (1 μg) and hence, the dose of nanoparticles decreased as their loading increased. These results indicate that the relative proportion of chitosan and pDNA within the nanoparticles is of high importance for the efficacy of gene expression. This is in accordance with the reported dependence of the charge ratio (i.e. relative amounts of chitosan to pDNA) on the efficacy of polyplex mediated gene delivery (Erbacher et al., 1998; Romoren et al., 2003). Furthermore, independent of the pDNA loading, the gene expression increased with time, thus peaking at around 8–10 days after transfection. This rather slow onset of gene expression obtained with the HMW nanoparticles agrees with the transfection behaviour of nanospheres and polyplexes based on HMW chitosan (Koping-Hoggard et al., 2001; Mao et al., 2001). To assure that a dose of 1 μg pDNA was adequate for the transfection response, the effect of the pDNA dose on the transfection efficiency was studied using 20% loaded HMW CS/TPP nanoparticles. Even at a dose of 0.5 μg pDNA, a high gene expression, but slightly lower than that obtained at 1 and 2 μg pDNA doses, was obtained (Fig. 4b). Based on these results a dose of 1 μg was chosen for all further *in vitro* transfection studies.

Next, the *in vitro* transfection of nanoparticles based on LMW chitosan was investigated. In contrast to nanoparticles based on HMW chitosan, LMW CS/TPP chitosan nanoparticles showed the highest transfection efficiency at a lower pDNA loading, i.e. 10% (Fig. 5a). This is in accordance with the reported behaviour of chitosan polyplexes that require a larger relative amount of chitosan vs. pDNA as the molecular weight of chitosan decreases (Koping-Hoggard et al., 2004; Romoren et al., 2003). Notably, the LMW CS/TPP nanoparticles gave high gene expression levels already at 2 days after transfection (around 27% GFP-positive cells), reaching a plateau of sustained high gene expression (around 35% GFP-positive cells) between 4 and 10 days, which differs from the delayed peak expression of the HMW chitosan nanoparticles. Furthermore, the nanoparticles based on LMW chitosan mediated higher gene expression than those based on HMW chitosan at all of the time points studied (Fig. 5b and c). This molecular weight dependence agrees well with results reported for chitosan–pDNA complexes (Sato et al., 2001). Interestingly, Janes et al. reported that insulin was more rapidly

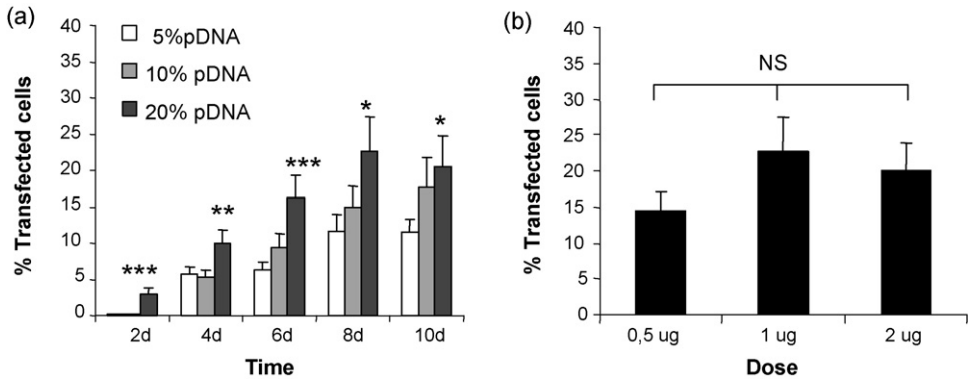

Fig. 4. Effect of (a) pDNA loading and (b) pDNA dose of HMW CS/TPP nanoparticles on GFP gene expression in HEK 293 cells. In (a) the dose was 1 μg pDNA per well and the cells were analyzed for up to 10 days. In (b) the pDNA loading was 20% and the cells were analyzed for GFP expression at day 8. Results are expressed as mean ± S.D. ($n = 3$). Statistical differences between 20 and 5% pDNA load are denoted as $^{*}P < 0.05$, $^{**}P < 0.01$ and $^{***}P < 0.001$, respectively. NS = no significant difference ($P > 0.05$).

released from LMW CS/TPP nanoparticles than insulin entrapped in nanoparticles formed from a higher molecular weight (Janes and Alonso, 2003). The faster release rate was presumably a result of the weaker interactions between the oligomeric chitosan and the encapsulated agent. Although pDNA displays a higher negative charge density than insulin, and consequently is not released into normal release medium whether encapsulated either into LMW or HMW CS/TPP nanoparticles (Fig. 2), the intracellular degradation of chitosan into oligomers and subsequent release of pDNA could be faster for shorter (LMW) chitosan chains than for longer ones (HMW). This could explain the faster onset of gene expression and the higher efficacy of LMW CS/TPP nanoparticles. In this case, this hypothesis is in accordance with the above-mentioned works that sustain the higher efficacy of LMW chitosan polyplexes compared to the HMW counterparts.

Chitosan–pDNA complexes (polyplexes) based on LMW chitosan were recently reported to be as efficient as polyplexes based on the synthetic polymer polyethylenimine (PEI), one of the most potent non-viral delivery systems, both in HEK 293 cells *in vitro* as after intratracheal administration to mice *in vivo* (Koping-Hoggard et al., 2004). To challenge the efficiency of the LMW CS/TPP nanoparticles, we compared the *in vitro* transfection efficiency to that obtained with LMW chitosan polyplexes. As shown in Fig. 5d, the nanoparticles mediated comparable gene expression levels as the polyplexes (around 35% GFP-positive cells). Thus, although the nanoparticles and polyplexes differed in the physical–chemical behaviour, their *in vitro* transfection behaviour was comparable. This indicates that the molecular weight of the carrier is a more important factor for efficient gene transfection rather than in which form (nanoparticles or polyplexes) it is presented to the cells *in vitro*. Still, the nanoparticles possess several interesting advantages compared to polyplexes such as (i) their higher physical and biological stability (De Campos et al., 2004; Vila et al., 2002), (ii) their ease of handling: possibility of isolation-resuspension, freeze-drying-reconstitution (Fernandez-Urrusuno et al., 1999b), and as discussed in the present work, (iii) the possibility of co-encapsulation and

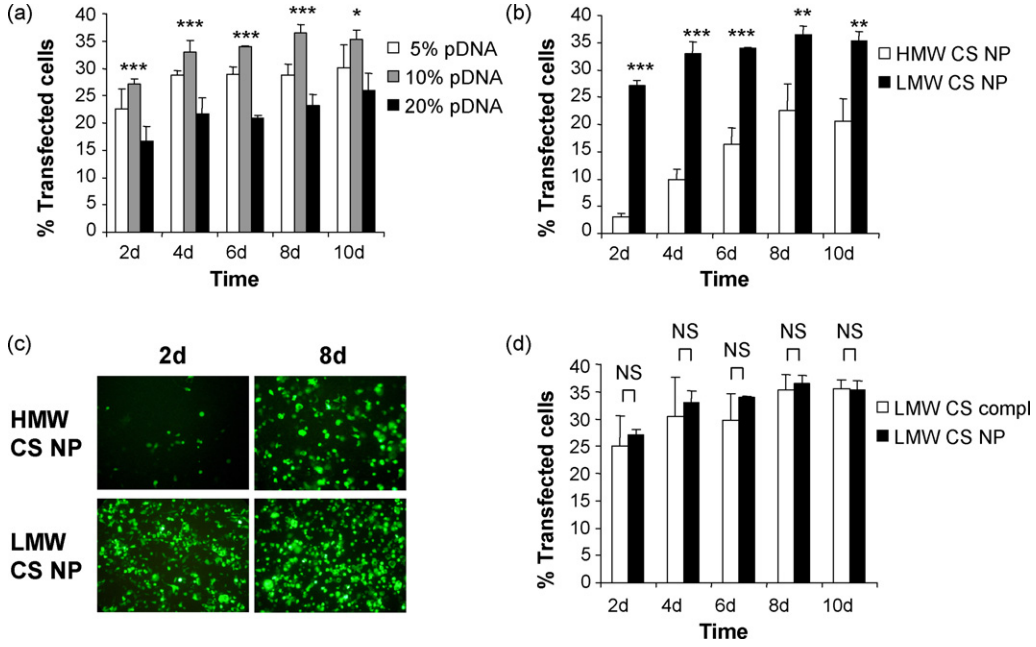

Fig. 5. Transfection efficiency of LMW CS/TPP nanoparticles. (a) Effect of pDNA loading on GFP gene expression in HEK 293 cells. A pDNA dose of 1 μg was used. (b and c) Comparison of GFP transfection efficiency between LMW and HMW CS/TPP nanoparticles at 10 and 20% pDNA loading, respectively and a dose of 1 μg pDNA. (d) Comparison of GFP transfection efficiency between LMW CS/TPP nanoparticles and complexes at 10% pDNA loading. In (a), (b) and (d) results are expressed as mean ± S.D. ($n = 3$). Statistical differences are denoted as $^{*}P < 0.05$, $^{**}P < 0.01$ and $^{***}P < 0.001$, respectively. NS = no significant difference ($P > 0.05$).

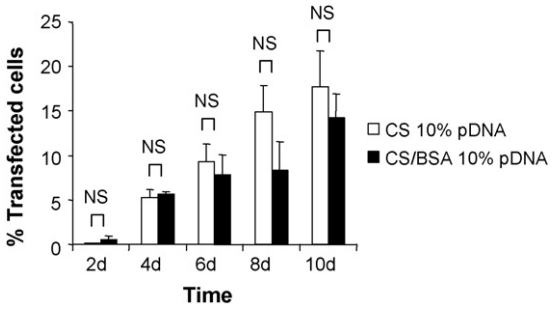

Fig. 6. GFP gene expression in HEK 293 cells transfected with HMW CS/TPP nanoparticles (10% pDNA load) with and without bovine serum albumin (BSA). A pDNA dose of 1 μg was used. Results are expressed as mean ± S.D. ($n = 3$). NS = no significant difference ($P > 0.05$).

controlled release of other molecules together with pDNA. Indeed, although the incorporation of BSA slightly decreased the pDNA loading capacity of the CS/TPP nanoparticles, the presence of BSA did not influence the inherent transfection capacity of the nanoparticles (Fig. 6). This demonstrates the potential for further improvements of the efficacy of CS/TPP nanoparticles through a co-encapsulating strategy with an active protein that could confer additional advantages to the nanoparticles such as improving the cell internalization or the intracellular trafficking of the plasmid DNA.

3.7. *In vitro* toxicity studies

The cell toxicity of CS/TPP nanoparticles and CS polyplexes was investigated by studying the dose-dependent effects on the metabolic activity in HEK 293 cells. As shown in Fig. 7a, the LMW CS/TPP nanoparticles (and polyplexes) showed no acute cell toxicity at concentrations used for transfections (9.09 μg/cm^2), in contrast to a slight decrease in cell viability with nanoparticles based on HMW chitosan. The LMW CS/TPP nanoparticles had higher IC_{50} (>36.4 μg/cm^2 cell surface) than the HMW CS/TPP nanoparticles (18 μg/cm^2 cell surface). However, after allowing the cells to recover for 24 h, the cells incubated with HMW chitosan nanoparticles regained the normal viability and no difference between the formulations could be detected. The difference in the immediate cellular response between HMW and LMW CS/TPP nanoparticles could be related to their different surface charge, i.e. zeta potential (Table 1). Thus, the greater positive zeta potential of the HMW CS/TPP nanoparticles, the stronger the interactions will be with the negatively charged cell membrane (Qi et al., 2005). However the cells regained normal viability within 24 h,

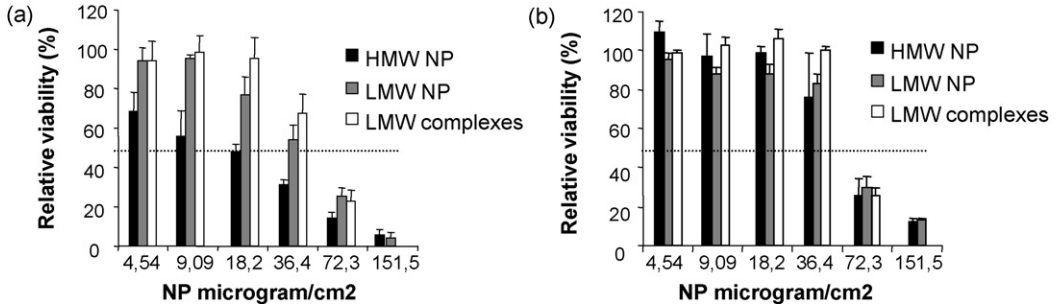

Fig. 7. MTS assay of *in vitro* toxicity using HMW CS/TPP nanoparticles and LMW CS/TPP nanoparticles and complexes in HEK 293 cells. The cells were assayed (a) immediately after removal of the formulations or (b) after recuperation for 24 h. The dotted line in (a) represents 50% relative viability. Results are expressed as mean ± S.D. ($n = 4$).

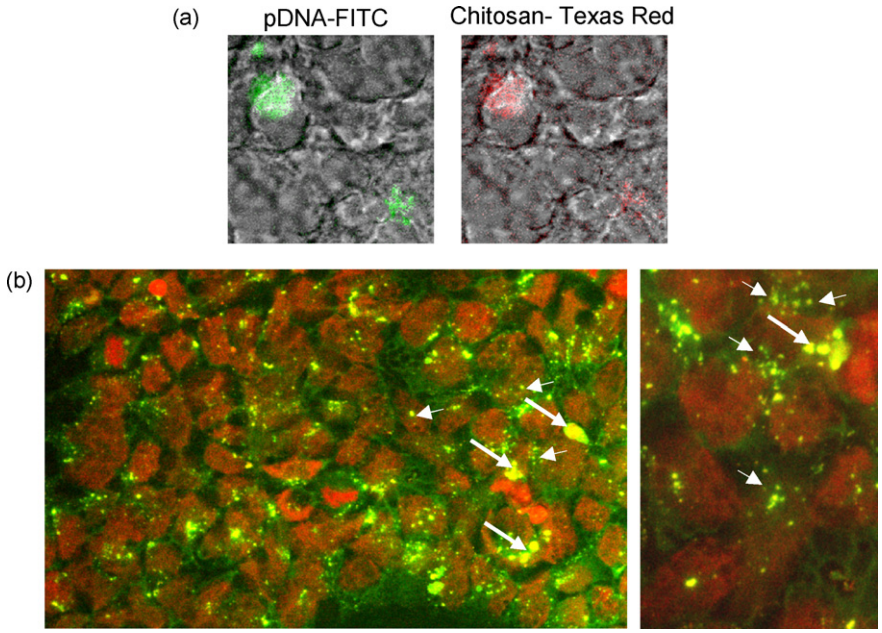

Fig. 8. Cellular uptake and intracellular distribution of LMW CS/TPP nanoparticles incubated with HEK 293 cells. (a) The chitosan-Texas red (red colour) and pDNA-FITC (green colour) are co-localized intracellularly in big vacuoles 1 h after transfection. (b) Plasmid DNA-FITC (green colour) is both localized in larger vacuoles (exemplified by large arrows) as well as in the cytoplasm (exemplified by small arrows) suggesting release of pDNA and/or nanoparticles from intracellular vacuoles.

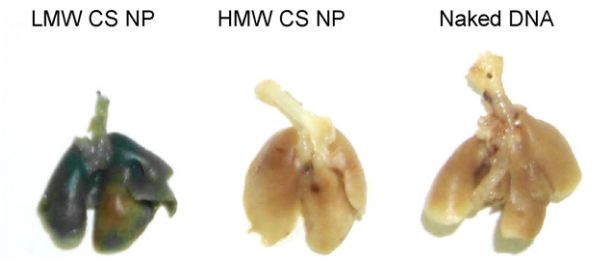

Fig. 9. Macroscopic evaluation of beta-galactosidase expression in mouse lungs. Lungs were analyzed 72 h after administration of LMW CS/TPP (10% pDNA loading) and HMW CS/TPP nanoparticles (20% pDNA loading) at a dose of 10 μg pCMV-βGal. Naked pCMV-βGal was used as control.

suggesting a transient effect of HMW chitosan on the cell viability (Fig. 7b).

3.8. Uptake and intracellular distribution of CS/TPP nanoparticles

In an attempt to get some information regarding the cellular uptake and intracellular fate of CS/TPP nanoparticles following transfection of HEK 293 cells, the intracellular distribution of fluorescently labelled LMW chitosan and/or pDNA was investigated by confocal fluorescence microscopy. For this purpose, we used chitosan labelled in red (Texas Red) and pDNA labelled in green (FITC). Cells were incubated with nanoparticles for 1 h and then examined either directly, or after 15 h post-incubation. As shown in Fig. 8a, 1 h after incubation chitosan and pDNA were already co-localized in the interior of the cells in large vacuolar compartments. This distribution pattern agrees with an endocytotic uptake of the nanoparticles, similar to that observed for DNA complexed with chitosan and its derivatives (Ishii et al., 2001; Yoo et al., 2005; Zhang et al., 2008). Moreover, the distribution showed a time-dependent profile as 14 h later fluorescent spots corresponding to both pDNA and chitosan could be also visualized in the cytoplasm, suggesting their release from the intracellular vacuoles (Fig. 8b). This release from the intracellular vacuoles following endocytosis is a prerequisite for efficient gene delivery and agrees with the high gene expression observed for LMW CS/TPP nanoparticles 24 h after transfection (as discussed in Section 3.6, Fig. 5).

3.9. Intratracheal administration of CS/TPP nanoparticles to mice

A qualitative assessment of the *in vivo* efficiencies of the LMW and HMW CS/TPP nanoparticles was obtained following intratracheal administration of nanoparticles loaded with pCMV-βGal to mice. As a control, naked pCMV-βGal was also administered. LMW CS/TPP nanoparticles mediated a strong beta-galactosidase gene expression in the mouse lungs 72 h post-administration in contrast to the HMW CS/TPP nanoparticles and naked pDNA (Fig. 9). The improved *in vivo* performance of the LMW CS/TPP nanoparticles as compared to that of HMW nanoparticles is in accordance with our *in vitro* transfection results (Fig. 5) and some of our recently published reports regarding chitosan:hyaluronan or chitosan:cyclodextrin nanoparticles prepared by an adapted ionotropic gelation method. In these cases, carriers based on chitosan oligomers were also found to be more efficient mucosal gene delivery systems than those made of HMW chitosan (De La Fuente et al., 2008a,b; Teijeiro-Osorio et al., 2009). Finally, as an alternative to the reduction of CS molecular weight, it is also interesting to mention that other studies carried out parallel in our group have indicated PEGylation as an efficient method for improving the performance HMW CS/TPP as gene carriers *in vitro* and *in vivo* (Csaba et al., 2009).

4. Conclusions

Ionically crosslinked CS/TPP nanoparticles represent an interesting alternative to other chitosan-based delivery systems for nucleic acids such as plasmid DNA or oligonucleotide sequences. While these carriers exhibit negligible toxicity, they mediate comparable gene expression levels to other, previously reported highly efficient gene delivery systems. In addition, CS:TPP nanoparticles are suitable for the simultaneous encapsulation and sustained release of other active molecules together with DNA. The results of the present study forward CS/TPP nanoparticles as a biocompatible non-viral gene delivery system and present a platform for further optimisation studies of chitosan-based nanoparticles, for example with regard to steric stabilization and targeting.

Acknowledgements

The studies were supported by grants from the Ministry of Sciences and Education of Spain (MAT2004-04792-C02-02) and the "Xunta de Galicia" (PGIDT03BTF20301PR) (Spain). We also would like to thank Mr. Rafael Romero for his technical assistance with the animal studies and confocal images.

References

Calvo, P., Remunan-Lopez, C., Vila-Jato, J.L., Alonso, M.J., 1997a. Chitosan and chitosan/ethylene oxide–propylene oxide block copolymer nanoparticles as novel carriers for proteins and vaccines. Pharm. Res. 14, 1431–1436.

Calvo, P., Remunan-Lopez, C., Vila Jato, J.L., Alonso, M.J., 1997b. Novel hydrophilic chitosan–polyethylene oxide nanoparticles as protein carriers. J. Appl. Polym. Sci. 63, 125–132.

Csaba, N., Caamano, P., Sanchez, A., Dominguez, F., Alonso, M.J., 2005. PLGA:poloxamer and PLGA:poloxamine blend nanoparticles: new carriers for gene delivery. Biomacromolecules 6, 271–278.

Csaba, N., Koping-Hoggard, M., Novoa-Carballal, R., Fernandez-Megia, E., Riguera, R., Alonso, M.J., 2009. Ionically crosslinked chitosan nanoparticles as gene delivery systems: effect of PEGylation degree on in vitro and in vivo gene transfer. J. Biomed. Nanotechnol. 71, 257–263.

Cuna, M., Alonso-Sandel, M., Remunan-Lopez, C., Pivel, J.P., Alonso-Lebrero, J.L., Alonso, M.J., 2006. Development of phosphorylated glucomannan-coated chitosan nanoparticles as nanocarriers for protein delivery. J. Nanosci. Nanotechnol. 6, 2887–2895.

Dang, J.M., Leong, K.W., 2006. Natural polymers for gene delivery and tissue engineering. Adv. Drug Deliv. Rev. 58, 487–499.

Danielsen, S., Varum, K.M., Stokke, B.T., 2004. Structural analysis of chitosan mediated DNA condensation by AFM: influence of chitosan molecular parameters. Biomacromolecules 5, 928–936.

De Campos, A.M., Diebold, Y., Carvalho, E.L., Sanchez, A., Alonso, M.J., 2004. Chitosan nanoparticles as new ocular drug delivery systems: in vitro stability, in vivo fate, and cellular toxicity. Pharm. Res. 21, 803–810.

De La Fuente, M., Seijo, B., Alonso, M.J., 2008a. Bioadhesive hyaluronan–chitosan nanoparticles can transport genes across the ocular mucosa and transfect ocular tissue. Gene Ther. 15, 668–676.

De La Fuente, M., Seijo, B., Alonso, M.J., 2008b. Novel hyaluronic acid–chitosan nanoparticles for ocular gene therapy. Invest. Ophthalmol. Vis. Sci. 49, 2016–2024.

Dung, T.H., Lee, S.R., Han, S.D., Kim, S.J., Ju, Y.M., Kim, et al., 2007. Chitosan–TPP nanoparticle as a release system of antisense oligonucleotide in the oral environment. J. Nanosci. Nanotechnol. 7, 3695–3699.

Erbacher, P., Zou, S., Bettinger, T., Steffan, A.M., Remy, J.S., 1998. Chitosan-based vector/DNA complexes for gene delivery: biophysical characteristics and transfection ability. Pharm. Res. 15, 1332–1339.

Fernandez-Megia, E., Novoa-Carballal, R., Quinoa, E., Riguera, R., 2005. Optimal routine conditions for the determination of degree of acetylation of chitosan by ^{1}H-NMR. Carbohydr. Polym. 61, 155–161.

Fernandez-Urrusuno, R., Calvo, P., Remunan-Lopez, C., Vila-Jato, J.L., Alonso, M.J., 1999a. Enhancement of nasal absorption of insulin using chitosan nanoparticles. Pharm. Res. 16, 1576–1581.

Fernandez-Urrusuno, R., Romani, D., Calvo, P., Vila Jato, J.L., Alonso, M.J., 1999b. Development of a freeze-dried formulation of insulin-loaded chitosan nanoparticles intended for nasal administration. STP Pharma Sci. 9, 429–436.

Howard, K.A., Paludan, S.R., Behlke, M.A., Besenbacher, F., Deleuran, B., Kjems, J., 2008. Chitosan/siRNA nanoparticle-mediated TNF-alpha knockdown in peritoneal macrophages for anti-inflammatory treatment in a murine arthritis model. Mol. Ther..

Howard, K.A., Rahbek, U.L., Liu, X., Damgaard, C.K., Glud, S.Z., Andersen, et al., 2006. RNA interference in vitro and in vivo using a novel chitosan/siRNA nanoparticle system. Mol. Ther. 14, 476–484.

Ishii, T., Okahata, Y., Sato, T., 2000. Facile preparation of a fluorescence-labeled plasmid. Biochim. Biophys. Acta 1514, 51–64.
Ishii, T., Okahata, Y., Sato, T., 2001. Mechanism of cell transfection with plasmid/chitosan complexes. Biochim. Biophys. Acta 1514, 51–64.
Janes, K., Alonso, M.J., 2003. Depolymerized chitosan nanoparticles for protein delivery: preparation and characterization. J. Appl. Polym. Sci. 12, 2769–2776.
Kiang, T., Bright, C., Cheung, C.Y., Stayton, P.S., Hoffman, A.S., Leong, K.W., 2004. Formulation of chitosan–DNA nanoparticles with poly(propyl acrylic acid) enhances gene expression. J. Biomater. Sci. Polym. Ed. 15, 1405–1421.
Kim, Y.H., Gihm, S.H., Park, C.R., Lee, K.Y., Kim, T.W., Kwon, I.C., et al., 2001. Structural characteristics of size-controlled self-aggregates of deoxycholic acid-modified chitosan and their application as a DNA delivery carrier. Bioconjug. Chem. 12, 932–938.
Koping-Hoggard, M., Mel'nikova, Y.S., Varum, K.M., Lindman, B., Artursson, P., 2003. Relationship between the physical shape and the efficiency of oligomeric chitosan as a gene delivery system in vitro and in vivo. J. Gene Med. 5, 130–141.
Koping-Hoggard, M., Tubulekas, I., Guan, H., Edwards, K., Nilsson, M., Varum, K.M., et al., 2001. Chitosan as a nonviral gene delivery system, Structure-property relationships and characteristics compared with polyethylenimine in vitro and after lung administration in vivo. Gene Ther. 8, 1108–1121.
Koping-Hoggard, M., Varum, K.M., Issa, M., Danielsen, S., Christensen, B.E., Stokke, B.T., et al., 2004. Improved chitosan-mediated gene delivery based on easily dissociated chitosan polyplexes of highly defined chitosan oligomers. Gene Ther. 11, 1441–1452.
Lamarque, G., Lucas, J.M., Viton, C., Domard, A., 2005. Physicochemical behavior of homogeneous series of acetylated chitosans in aqueous solution: role of various structural parameters. Biomacromolecules 6, 131–142.
Lee, D., Zhang, W., Shirley, S.A., Kong, X., Hellermann, G.R., Lockey, R.F., et al., 2007. Thiolated chitosan/DNA nanocomplexes exhibit enhanced and sustained gene delivery. Pharm. Res. 24, 157–167.
Leong, K.W., Mao, H.Q., Truong-Le, V.L., Roy, K., Walsh, S.M., August, J.T., 1998. DNA–polycation nanospheres as non-viral gene delivery vehicles. J. Control Release 53, 183–193.
Liu, X., Howard, K.A., Dong, M., Andersen, M.O., Rahbek, U.L., Johnsen, et al., 2007. The influence of polymeric properties on chitosan/siRNA nanoparticle formulation and gene silencing. Biomaterials 28, 1280–1288.
Mansouri, S., Lavigne, P., Corsi, K., Benderdour, M., Beaumont, E., Fernandes, J.C., 2004. Chitosan–DNA nanoparticles as non-viral vectors in gene therapy: strategies to improve transfection efficacy. Eur. J. Pharm. Biopharm. 57, 1–8.
Mao, H.Q., Roy, K., Troung-Le, V.L., Janes, K.A., Lin, K.Y., Wang, Y., et al., 2001. Chitosan–DNA nanoparticles as gene carriers: synthesis, characterization and transfection efficiency. J. Control Release 70, 399–421.
Morille, M., Passirani, C., Vonarbourg, A., Clavreul, A., Benoit, J.P., 2008. Progress in developing cationic vectors for non-viral systemic gene therapy against cancer. Biomaterials 29, 3477–3496.
Qi, L., Xu, Z., Jiang, X., Li, Y., Wang, M., 2005. Cytotoxic activities of chitosan nanoparticles and copper-loaded nanoparticles. Bioorg. Med. Chem. Lett. 15, 1397–1399.
Romoren, K., Pedersen, S., Smistad, G., Evensen, O., Thu, B.J., 2003. The influence of formulation variables on in vitro transfection efficiency and physicochemical properties of chitosan-based polyplexes. Int. J. Pharm. 261, 115–127.
Sato, T., Ishii, T., Okahata, Y., 2001. In vitro gene delivery mediated by chitosan. Effect of pH, serum, and molecular mass of chitosan on the transfection efficiency. Biomaterials 22, 2075–2080.
Teijeiro-Osorio, D., Remunan-Lopez, C., Alonso, M.J., 2009. Chitosan/cyclodextrin nanoparticles can efficiently transfect the airway epithelium in vitro. Eur. J. Pharm. Biopharm. 71, 257–263.
Vila, A., Sanchez, A., Tobio, M., Calvo, P., Alonso, M.J., 2002. Design of biodegradable particles for protein delivery. J. Control Release 78, 15–24.
Yoo, H.S., Lee, J.E., Chung, H., Kwon, I.C., Jeong, S.Y., 2005. Self-assembled nanoparticles containing hydrophobically modified glycol chitosan for gene delivery. J. Control Release 103, 235–243.
Zhang, H., Oh, M., Allen, C., Kumacheva, E., 2004. Monodisperse chitosan nanoparticles for mucosal drug delivery. Biomacromolecules 5, 2461–2468.
Zhang, X., Ercelen, S., Duportail, G., Schaub, E., Tikhonov, V., Slita, A., et al., 2008. Hydrophobically modified low molecular weight chitosans as efficient and non-toxic gene delivery vectors. J. Gene Med. 10, 527–539.